

Ultrafast spin-switching of a ferrimagnetic alloy at room temperature traced by resonant magneto-optical Kerr effect using a seeded free electron laser

Sh. Yamamoto, M. Taguchi, T. Someya, Y. Kubota, S. Ito, H. Wadati, M. Fujisawa, F. Capotondi, E. Pedersoli, M. Manfreda, L. Raimondi, M. Kiskinova, J. Fujii, P. Moras, T. Tsuyama, T. Nakamura, T. Kato, T. Higashide, S. Iwata, S. Yamamoto, S. Shin, and I. Matsuda

Citation: *Review of Scientific Instruments* **86**, 083901 (2015); doi: 10.1063/1.4927828

View online: <http://dx.doi.org/10.1063/1.4927828>

View Table of Contents: <http://scitation.aip.org/content/aip/journal/rsi/86/8?ver=pdfcov>

Published by the [AIP Publishing](#)

Articles you may be interested in

[Effect of damping on the laser induced ultrafast switching in rare earth-transition metal alloys](#)

Appl. Phys. Lett. **104**, 222404 (2014); 10.1063/1.4881135

[Precessional switching by ultrashort pulse laser: Beyond room temperature ferromagnetic resonance limit](#)

J. Appl. Phys. **109**, 07D302 (2011); 10.1063/1.3535415

[Field-dependent ultrafast dynamics and mechanism of magnetization reversal across ferrimagnetic compensation points in GdFeCo amorphous alloy films](#)

J. Appl. Phys. **108**, 023902 (2010); 10.1063/1.3462429

[A setup combining magneto-optical Kerr effect and conversion electron Mössbauer spectrometry for analysis of the near-surface magnetic properties of thin films](#)

Rev. Sci. Instrum. **80**, 043905 (2009); 10.1063/1.3121215

[Time-resolved Kerr measurements of magnetization switching in a crossed-wire ferromagnetic memory element](#)

J. Appl. Phys. **91**, 7331 (2002); 10.1063/1.1452681

oerlikon
leybold vacuum

online shop
now available
in 12 countries



Vacuum Technology Made Easy

www.leyboldvacuum-shop.com

Ultrafast spin-switching of a ferrimagnetic alloy at room temperature traced by resonant magneto-optical Kerr effect using a seeded free electron laser

Sh. Yamamoto,¹ M. Taguchi,² T. Someya,¹ Y. Kubota,¹ S. Ito,¹ H. Wadati,¹ M. Fujisawa,¹ F. Capotondi,³ E. Pedersoli,³ M. Manfredda,³ L. Raimondi,³ M. Kiskinova,³ J. Fujii,⁴ P. Moras,⁵ T. Tsuyama,¹ T. Nakamura,^{1,6} T. Kato,⁷ T. Higashide,⁷ S. Iwata,⁸ S. Yamamoto,¹ S. Shin,¹ and I. Matsuda^{1,a)}

¹*Institute for Solid State Physics, The University of Tokyo, 5-1-5 Kashiwanoha, Kashiwa, Chiba 277-8581, Japan*

²*Nara Institute of Science and Technology (NAIST), Ikoma, Nara 630-0192, Japan*

³*Elettra-Sincrotrone Trieste, SS 14 - km 163.5, I-34149 Basovizza, Trieste, Italy*

⁴*Laboratorio TASC, Istituto Officina dei Materiali, Consiglio Nazionale delle Ricerche, I-34012 Basovizza, Trieste, Italy*

⁵*Istituto di Struttura della Materia, Consiglio Nazionale delle Ricerche, Trieste, Italy*

⁶*Japan Synchrotron Radiation Research Institute/SPring-8, Sayo, Hyogo 679-5198, Japan*

⁷*Department of Electrical Engineering and Computer Science, Nagoya University, Chikusa, Nagoya 464-8603, Japan*

⁸*Division of Integrated Research Projects, EcoTopia Science Institute, Nagoya University, Chikusa, Nagoya 464-8603, Japan*

(Received 5 July 2015; accepted 20 July 2015; published online 7 August 2015)

Ultrafast magnetization reversal of a ferrimagnetic metallic alloy GdFeCo was investigated by time-resolved resonant magneto-optical Kerr effect measurements using a seeded free electron laser. The GdFeCo alloy was pumped by a linearly polarized optical laser pulse, and the following temporal evolution of the magnetization of Fe in GdFeCo was element-selectively traced by a probe free electron laser pulse with a photon energy tuned to the Fe *M*-edge. The results have been measured using rotating analyzer ellipsometry method and confirmed magnetization switching caused by ultrafast heating. © 2015 Author(s). All article content, except where otherwise noted, is licensed under a Creative Commons Attribution 3.0 Unported License. [<http://dx.doi.org/10.1063/1.4927828>]

Ultrafast spin dynamics in femtosecond time scale, the so-called femtomagnetism, has been one of the central issues in the frontier of science and technology for the last two decades.^{1,2} To capture the nature of the non-equilibrium dynamics, ultrafast time-resolved experiments have been carried out using ultra-short laser pulses. Recently, the development of EUV-X-ray free electron lasers (FELs) and high harmonic generation (HHG) lasers has opened the opportunity for exploring dynamic phenomena with element selectivity by tuning the photon energy of the laser pulses to the absorption edges of material constituents. Since the fundamental origin of the magnetism is the electron exchange interactions, which occur in femtosecond time scales, ultrafast experiments using FELs and HHG lasers are expected to add the missing knowledge in condensed matter physics for pushing technological innovation in ultrafast spintronics.

The well-known magnetization reversal of GdFeCo ferrimagnetic alloy was first observed by time-resolved visible magneto-optical Kerr effect (MOKE) measurements.³ In this earlier study, the magnetization reversal occurred on a time scale longer than 100 ps as a result of temperature- and field-induced effects. GdFeCo is a ferrimagnetic metallic alloy, composed of rare-earth (RE) and transition metal (TM) sublattices that couple anti-ferromagnetically. After Kimel *et al.*⁴ showed that a helicity of excitation laser pulse can affect the

state of magnetization, light-matter interaction has attracted our attention. Helicity-dependent magnetization reversal of GdFeCo, using circularly polarized light as an effective magnetic field, has already been observed (so-called opto-magnetic effect).⁵ Only later, all-optical switching has been observed without applying an external magnetic field using circularly polarized light^{6,7} or even linearly polarized light.^{8–10} Recently, all-optical helicity-dependent switching of ferromagnetic materials has been perceived as well.¹¹ Many models have been proposed to describe the microscopic origin of magnetization reversal in ferrimagnetic materials, such as Inverse Faraday effect (IFE),¹² the combination of IFE with ultrafast heating,¹³ ferromagnetic-like coupling between two non-equivalent sublattices due to the nonequilibrium nature,⁸ transfer of angular momentum between two sublattices' coupling via antiferromagnetic exchange interaction,^{14,15} and superdiffusive current.¹⁶ Dynamical path for magnetization reversal is also still disputable, whether it is only involved with longitudinal modulus of magnetization or not.¹⁷ Therefore, the mechanism of magnetization switching of ferrimagnetic systems is still unclear and controversial so far. In this letter, we focus on magnetization reversal of GdFeCo using linearly polarized light in terms of thermal effect, which excludes the non-thermal one such as IFE.

Figures 1(a) and 1(b) compare the previous reports on the Fe magnetization switching induced by the linearly polarized light, under various experimental conditions.^{8,9} As shown in Fig. 1(a), in the time-resolved X-ray magnetic circular

^{a)}Electronic mail: imatsuda@issp.u-tokyo.ac.jp



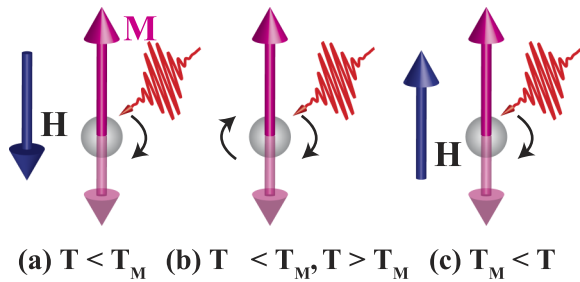


FIG. 1. Comparison of experimental configurations in ultrafast magnetization reversal among (a) Ref. 8, (b) Ref. 9, and (c) this study; up-pointing red arrow shows direction of Fe magnetization before irradiation, in (a) and (c) the down-pointing blue arrow is an external magnetic field and the black curved arrow shows the way the magnetization reverses by the linearly polarized pumping laser. The temperature shown at the lower part in each diagram represents the comparison with the T_M before pumping.

dichroism (XMCD) experiment using laser-slicing source,⁸ the external field was applied before pumping antiparallel to the Fe magnetization. In the hundreds of femtoseconds, the Fe magnetization reverses to the direction of the applied magnetic field through the transient ferromagnetic-like Gd-Fe state. The sample temperature was initially set below the magnetic compensation temperature, T_M , at which the net magnetization of the ferrimagnet becomes zero. Figure 1(b) shows the result of a time-resolved XMCD-photoemission electron microscopy experiment.⁹ Here, in contrast to the case in Fig. 1(a), the Fe magnetization switching was observed without applying external magnetic field and at temperatures both above and below T_M before pumping. It is obvious that more information about the effects of the sample temperature and the external magnetic field on the ultrafast magnetization switching caused mainly by heating is necessary. In the present study, we adopted the third experimental condition, shown in Fig. 1(c). Before pumping, the sample was set at room temperature, which is above the GdFeCo $T_M \sim 250$ K. The external magnetic field was applied in the direction of the initial Fe magnetization. The femtosecond time-resolved measurement of the resonant MOKE (RMOKE) was carried out using the seeded FEL pulses as a probe. Compared to visible MOKE, distinct features of RMOKE are the large magneto-optical response,¹⁸ element selectivity, the selection of light polarization, and also the possibility for combining with other methods, e.g., diffraction with the same experimental set-up. In the present study, the Fe magnetization reversal in real time was measured tuning the photon energy to the Fe M -absorption edge, to achieve element-selectivity.

Figure 2(a) shows a schematic diagram of the thin-film sample structure, where the ferrimagnetic alloy has the composition $\text{Gd}_{21}(\text{Fe}_{90}\text{Co}_{10})_{79}$. The $T_M \sim 250$ K of the $\text{Gd}_{21}(\text{Fe}_{90}\text{Co}_{10})_{79}$ is lower than room temperature. For this alloy composition, the magnetic moment at room temperature of the TM sublattice is higher than the RE one and the direction of the magnetic moment of the Fe atom is parallel to that of the external magnetic field. A multilayer film of Ta (2 nm)/GdFeCo (20 nm)/Ta (10 nm) was fabricated on thermally oxidized silicon wafers using RF magnetron sputtering. The Ta (2 nm) capping layer prevents the GdFeCo oxidization and the Ta (10 nm) underlayer helps the

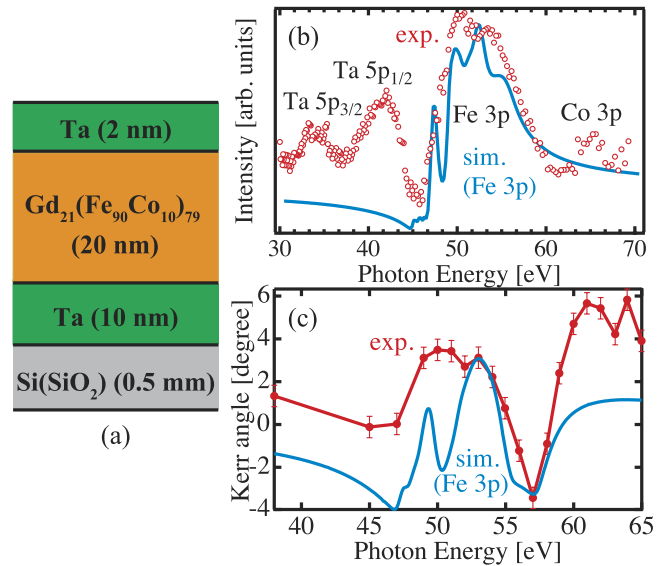


FIG. 2. (a) A schematic diagram of a 20-nm-thick GdFeCo film. (b) XAS spectra of the GdFeCo film calculated (sim.) and measured experimentally (exp.) using TEY mode. (c) The photon energy dependence of the Kerr rotation angle, θ_K . Measurement was performed at room temperature under a magnetic field of $B = \pm 0.47$ T. In calculation, the resonant effect of Fe 3p edge was taken into account and the effect of Ta 5p- and Co 3p-edges was not considered.

adhesion to the Si substrate. Figure 2(b) shows a set of X-ray absorption spectroscopy (XAS) spectra for the GdFeCo sample under the saturated magnetization condition. The red circles denote the experimental results obtained by the total electron yield (TEY) mode and the peak at 33 eV, 42 eV, and 66 eV is assigned to the Ta $5p_{3/2}$, $5p_{1/2}$, and Co 3p absorption, respectively. This measurement was carried out at the bending-magnet beamline BL-5B at UVSOR (Japan). The blue line represents the calculated Fe 3p XAS spectra based on a configuration interaction (CI) model,¹⁸ showing good agreement with the experiment. Figure 2(c) compares experimentally measured and calculated RMOKE spectra around the Fe M -absorption edge. The RMOKE measurements were conducted in polar geometry, where an external field (± 0.47 T) was applied perpendicular to the sample surface. The measurement geometry of static RMOKE was exactly the same as that of time-resolved RMOKE (TR-RMOKE) with FEL, described in detail below. Values of the Kerr rotation angle were obtained by the rotating analyzer ellipsometry (RAE) method, as illustrated in the inset of Figure 3. The details of the measurement system are described elsewhere.¹⁸ The RMOKE simulation¹⁸ was made for the same experimental geometry using the magnetic parameters obtained from the XMCD spectra taken at the undulator beamline BL-16A at Photon Factory (Japan). Using the sum-rules, the orbital magnetic moment (m_{orb}) and spin magnetic moment (m_{spin}) of the sample were evaluated to be $m_{orb} = 0.50$ and $m_{spin} = 2.33 \mu_B/\text{atom}$, respectively. In Fig. 2(c), the differences between the experiment and simulation are ascribed to the resonant effect of Co around 60 eV and to the optical interference effect of the nanometer thick film (not considered in the calculation) around 40 eV.^{18,19} From a set of the XAS and RMOKE data, photon energy of 53 eV is found to be the most suitable for tracing the magnetization dynamics

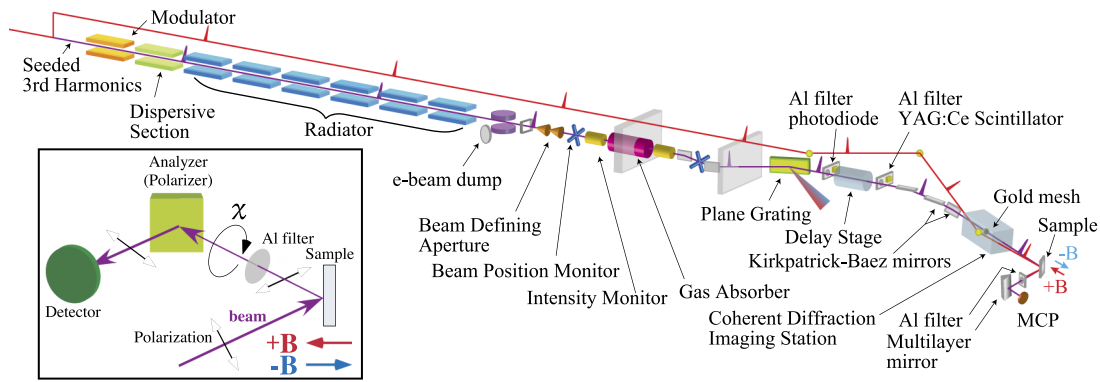


FIG. 3. Overview of the seeded-type FEL, DiProI beamline (FERMI@ELETTRA) with a femtoseconds-pulse pump which also acts as a seed for FEL and a measurement system for RAE. Our measurement chamber was connected at the end of the coherent diffraction imaging station in series. (Inset) Details of the RAE unit composed of a Mo/Si multilayer used for an analyzer and a detector, microchannel plate. In the RMOKE measurement, a polarizer-detector pair rotates on an axis connecting the analyzer and the sample.

of the Fe atom in the GdFeCo during the ultrafast switching in the present time-resolved measurement.

Figure 3 shows an overview of the TR-RMOKE measurement system with the probing seeded FEL and the pumping infrared (IR) lasers. The measurements were carried out at room temperature, using the DiProI beamline²⁰ at seeded FERMI FEL at Elettra laboratory in Italy. We used the FEL-1, which is normally operated at 60–20 nm ($h\nu = 12.4\text{--}62$ eV) with an electron beam energy of 1.2 GeV.^{21,22} Compared to the commonly used self-amplified spontaneous emission (SASE) scheme, FERMI that uses a HGHG seeding scheme has excellent longitudinal coherence and spectral purity and is also offering multiple polarized pulses.²³ Furthermore, since FERMI is a laser-seeded FEL, the same IR laser, intrinsically synchronized with the FEL pulses, can be used for practically jitter-free time resolved experiments.²⁴

In the present measurements, we used as a probe 80–100 fs FERMI pulses tuned to 23.6 nm (52.5 eV), generated with repetition rate of 10 Hz, and as a pump a 780 nm IR laser. The FEL and IR laser beams on to the sample had spot-size of diameters 420 μm and 530 μm , respectively. The time resolution is limited by the pulse widths of the pump laser, 150 fs. The fluence of the pump and the probe pulses was tuned to 14 mJ/cm^2 and 3 mJ/cm^2 , respectively. The temporal overlap of these pulses was determined within ± 50 ps, using a signal generated on a specially designed copper antenna connected through a high bandwidth coax cable to a fast oscilloscope²⁴ and the spatial overlapping by a YAG crystal. After setting the temporal overlap, we determined time zero with 250 fs resolution by monitoring the reflectivity changes of Si_3N_4 in classical FEL-pump/IR-laser-probe experiment.^{24,25}

Concerning the experimental configuration, the linear-horizontally polarized IR beam and the linear-vertically polarized FEL beam were coaxially incident onto the sample. The FEL irradiated the sample in the *s*-polarization configuration. The angles of the incident and reflected probe FEL beams were set at 45° with respect to the surface normal. The reflected FEL beam travelled to the polarizer, composed of a rotary flange, a Mo/Si multilayer mirror (10 periods of a 19.1 nm layer), and MCP as a detector of reflected light. The reflected IR laser was attenuated by an Al filter. The ellipsometry was conducted by

rotating the RAE unit. The principle of determination of Kerr rotation angle at each delay time was same as those used in the static RMOKE measurement. The fluctuating pulse to pulse intensity of the FERMI pulses was monitored in a shot-by-shot manner using a gas cell.

Figure 4(a) shows the results of time-resolved measurements. Each panel shows the RAE results at each indicated delay time. The vertical axis denotes the normalized intensity, i.e., the intensity detected at MCP divided by the incident intensity. The intensity of the light, reflected by the analyzer, is monitored at the detector as a function of χ , as shown in the inset of Fig. 3. The two curves (blue and red) correspond to the measurements under the applied magnetic field in up and down directions along the sample surface normal. The solid lines are cosine fitting to the experimental results, which is normalized so as to be consistent between two curves. The angle zero in each panel corresponds to the extinction state without external field. The Kerr rotation angle at each delay time can be extracted from the phase difference between the two curves. The initial Kerr rotation angle of 3.1° , measured in the static RMOKE (see Fig. 2), was reproduced in time-resolved measurements tuning the FEL energy to 53 eV at -100 fs, at which the Kerr rotation angle is 3.2° . Since a polar geometry is used in this TR-RMOKE measurement, the Kerr rotation angle indicates the out-of-plane magnetic moment of Fe in GdFeCo. Figure 4(b) schematically depicts the magnetization dynamics with respect to the external field resulting from the time dependent Kerr rotation angle. The length of the arrows in the figure corresponds to the magnitude of the Kerr rotation angle for each delay time. 200 fs after the intense laser irradiation, the changes of sign of the Kerr rotation angle indicate reversal of Fe magnetization. This reversal mechanism is classified in thermal process, different from the process involving IFE in the previous studies using circularly polarized beam.⁵ Considering the FERMI-FEL repetition rate of 10 Hz, the Fe magnetic moment is recovered at least 100 ms after the pump. Since linearly polarized IR pump laser was used, there is no coupling in terms of the exchange of angular momentum between photons and spins in the material. This means that the path for angular momentum transfer is closed between the sub-lattices of Gd and Fe.¹⁴ The time scale

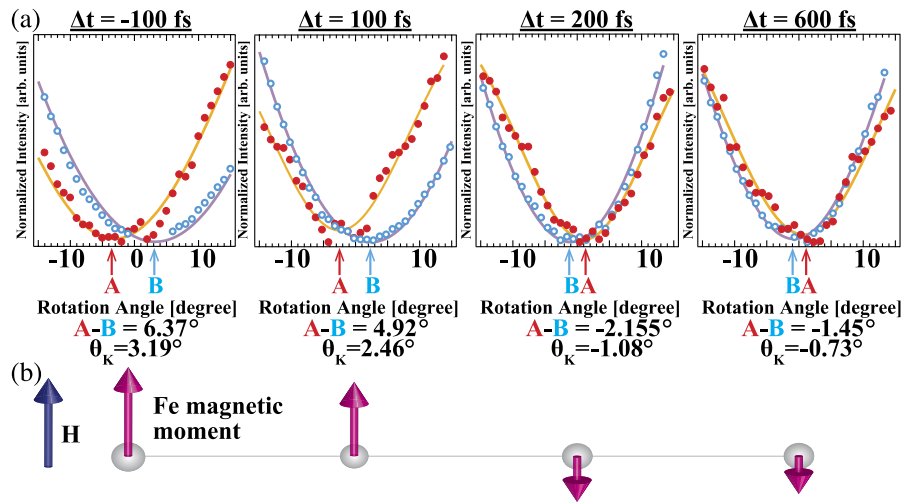


FIG. 4. (a) Experimental results (circles) of the intensity variation with rotation angle taken at $h\nu = 53$ eV for FEL for different delay time, shown in each panel with fitting by cosine curve (solid lines). (b) A schematic diagram of the magnetization reversal dynamics of the Fe magnetic moment with respect to an external field H . The length of the arrows is scaled to the magnitude of the Kerr rotation angle at each delay time shown in (a).

of magnetization reversal of TM sublattice is the same as observed in preceding research using time-resolved XMCD (TR-XMCD), in which transient ferromagnetic-like coupling has been observed due to different demagnetization times for RE and TM sublattices.^{8,9} Our measurement of TR-RMOKE reveals its compatibility with FEL for tracing ultrafast spin dynamics.

Concerning methodological approach, MOKE in the visible region is widely used for tracing spin dynamics of an average magnetization of a magnetic medium.²⁷ In the present paper, we report the advantage of RMOKE that allows for tracing ultrafast spin dynamics with element selectivity. In static XMCD measurements, largely conducted at synchrotron radiation facilities, detecting the absorption, reflection, or fluorescence yield, spin and orbital magnetic moment combining with sum rules have been probed.²⁶ Until now, the experiments using linearly polarized pumping light in an element-selective way have been conducted applying TR-XMCD in reflection. Fundamentally, both RMOKE and XMCD originate from the same principle, namely, the difference of absorption between right- and left-circularly polarized light by a magnetic medium that has spin-orbit and exchange splitting. In pump-probe measurements, photon-in/photon-out setup is utilized by both methods and can be used to scan a depth profile by changing incident angle to a layered structure or multilayer sample.¹ However, compared to the intensity measurements in XMCD, the polarization analysis in RMOKE can be used to extract the complete set of magneto-optical constants (dispersive and absorptive component of refractive indices) in a single experiment.²⁸ Furthermore, for polarization analysis of RMOKE we utilized the RAE method, in which small amount of change of Kerr angle can be detected because at each delay time ellipsometry was conducted and the Kerr angle was measured from the phase difference under two external magnetic fields (see Fig. 4(a)).¹⁸ In the static experiment, shown in Figure 2(c) for RMOKE, we observed that around the Fe M edge at 53 eV the Kerr rotation angle is nearly constant against energy between 3° and 4°. Therefore, TR-RMOKE of GdFeCo is more compatible with FEL

than using XMCD. It should be noted that in time-resolved MOKE measurements, it has been argued that the MOKE signal is modified by a non-equilibrium state generated during the femtosecond pulse so that the MOKE signal does not reflect the sample magnetization.²⁹ Since the delay time of the present experiment was much longer than the dephasing time of coherent correlation between photons and spins, the modulation effect can be neglected in interpreting the spin dynamics.

In conclusion, we measured the magnetization reversal of Fe in GdFeCo alloy within several 100 fs using a seeded-FEL tuned to the Fe M -absorption edge. The results are compared with the calculations based on the resonant scattering theory. Our results have revealed the magnetization switching due to ultrafast heating effect and demonstrate that studies combining FEL and TR-RMOKE experiments are opening new possibilities for investigating ultrafast magnetism.

This work was partially supported by the Ministry of Education, Culture, Sports, Science, and Technology of Japan (X-ray Free Electron Laser Priority Strategy Program and Photon and Quantum Basic Research Coordinated Development Program) and the Asahi Glass Foundation. The preliminary experiment was carried out by the joint research in the Synchrotron Radiation Research Organization and the Institute for Solid State Physics, the University of Tokyo (Proposal Nos. 2013B7453, 2014A7401, and 2014A7461). Sample characterization was performed at Photon Factory (Proposal No. 2013G058) and UVSOR (Proposal No. 26-564). The DiProI beamline was funded by the FERMI project of Elettra-Sincrotrone Trieste, partially supported by the Ministry of University and Research under grant numbers FIRB-RBAP045JF2 and FIRB-RBAP06AWK3 and by the grant from Friuli Venezia Giulia Region: Nanotox 0060-2009.

¹J. Stöhr and H. C. Siegmann, *Magnetism: From Fundamentals to Nanoscale Dynamics* (Springer, Berlin, Heidelberg, 2006).

²A. Kirilyuk, A. V. Kimel, and Th. Rasing, *Rev. Mod. Phys.* **82**, 2731 (2010).

³J. Hohlfield, Th. Gerrits, M. Bilderbeek, Th. Rasing, H. Awano, and N. Ohta, *Phys. Rev. B* **65**, 012413 (2001).

- ⁴A. V. Kimel, A. Kirilyuk, P. A. Usachev, R. V. Pisarev, A. M. Balbashov, and Th. Rasing, *Nature* **435**, 655 (2005).
- ⁵C. D. Stanciu, F. Hansteen, A. V. Kimel, A. Kirilyuk, A. Tsukamoto, A. Itoh, and Th. Rasing, *Phys. Rev. Lett.* **99**, 047601 (2007).
- ⁶C. D. Stanciu, A. Tsukamoto, A. V. Kimel, F. Hansteen, A. Kirilyuk, A. Itoh, and Th. Rasing, *Phys. Rev. Lett.* **99**, 217204 (2007).
- ⁷K. Vahaplar, A. M. Kalashnikova, A. V. Kimel, S. Gerlach, D. Hinzke, U. Nowak, R. Chantrell, A. Tsukamoto, A. Itoh, A. Kirilyuk, and Th. Rasing, *Phys. Rev. B* **85**, 104402 (2012).
- ⁸I. Radu, K. Vahaplar, C. Stamm, T. Kachel, N. Pontius, H. A. Dürr, T. A. Ostler, J. Barker, R. F. L. Evans, R. W. Chantrell, A. Tsukamoto, A. Itoh, A. Kirilyuk, Th. Rasing, and A. V. Kimel, *Nature* **472**, 205 (2011).
- ⁹T. A. Ostler, J. Barker, R. F. L. Evans, R. W. Chantrell, U. Atxitia, O. Chubykalo-Fesenko, S. El Moussaoui, L. Le Guyader, E. Mengotti, L. J. Heyderman, F. Nolting, A. Tsukamoto, A. Itoh, D. Afanasiev, B. A. Ivanov, A. M. Kalashnikova, K. Vahaplar, J. Mentink, A. Kirilyuk, Th. Rasing, and A. V. Kimel, *Nat. Commun.* **3**, 666 (2012).
- ¹⁰A. R. Khorsand, M. Savoini, A. Kirilyuk, A. V. Kimel, A. Tsukamoto, A. Itoh, and Th. Rasing, *Phys. Rev. Lett.* **110**, 107205 (2013).
- ¹¹C.-H. Lambert, S. Mangin, B. S. D. Ch. S. Varaprasad, Y. K. Takahashi, M. Hehn, M. Cinchetti, G. Malinowski, K. Hono, Y. Fainman, M. Aeschlimann, and E. E. Fullerton, *Science* **345**, 1337 (2014).
- ¹²F. Hansteen, A. V. Kimel, A. Kirilyuk, and Th. Rasing, *Phys. Rev. Lett.* **95**, 047402 (2005).
- ¹³K. Vahaplar, A. M. Kalashnikova, A. V. Kimel, D. Hinzke, U. Nowak, R. Chantrell, A. Tsukamoto, A. Itoh, A. Kirilyuk, and Th. Rasing, *Phys. Rev. Lett.* **103**, 117201 (2009).
- ¹⁴J. H. Mentink, J. Hellsvik, D. V. Afanasiev, B. A. Ivanov, A. Kirilyuk, A. V. Kimel, O. Eriksson, M. I. Katsnelson, and Th. Rasing, *Phys. Rev. Lett.* **108**, 057202 (2012).
- ¹⁵A. Baral and H. C. Schneider, *Phys. Rev. B* **91**, 100402 (2015).
- ¹⁶M. Battiato, K. Carva, and P. M. Oppeneer, *Phys. Rev. Lett.* **105**, 027203 (2010).
- ¹⁷S. Wienholdt, D. Hinzke, K. Carva, P. M. Oppeneer, and U. Nowak, *Phys. Rev. B* **88**, 020406 (2013).
- ¹⁸Sh. Yamamoto, M. Taguchi, M. Fujisawa, R. Hobar, S. Yamamoto, K. Yaji, T. Nakamura, K. Fujikawa, R. Yukawa, T. Togashi, M. Yabashi, M. Tsunoda, S. Shin, and I. Matsuda, *Phys. Rev. B* **89**, 064423 (2014).
- ¹⁹S. Valencia, H.-Ch. Mertins, D. Abramsohn, A. Gaupp, W. Gudat, and P. M. Oppeneer, *Physica B* **345**, 189 (2004).
- ²⁰F. Capotondi, E. Pedersoli, N. Mahne, R. H. Menk, G. Passos, L. Raimondi, C. Svetina, G. Sandrin, M. Zangrando, M. Kiskinova, S. Bajt, M. Barthelmess, H. Fleckenstein, H. N. Chapman, J. Schulz, J. Bach, R. Frömter, S. Schleitzer, L. Müller, C. Gutt, and G. Grübel, *Rev. Sci. Instrum.* **84**, 051301 (2013).
- ²¹E. Allaria, R. Appio, L. Badano, W. A. Barletta, S. Bassanese, S. G. Biedron, A. Borgia, E. Busetto, D. Castronovo, P. Cinquegrana, S. Cleva, D. Cocco, M. Cornacchia, P. Craievich, I. Cudin, G. D'Auria, M. Dal Forno, M. B. Danailov, R. De Monte, G. De Ninno, P. Delgiusto, A. Demidovich, S. Di Mitri, B. Diviacco, A. Fabris, R. Fabris, W. Fawley, M. Ferianis, E. Ferrari, S. Ferry, L. Froehlich, P. Fulran, G. Gaio, F. Gelmetti, L. Giannessi, M. Giannini, R. Gobessi, R. Ivanov, E. Karantzoulis, M. Lonza, A. Lutman, B. Mahieu, M. Milloch, S. V. Milton, M. Musardo, I. Nikolov, S. Noe, F. Parmigiani, G. Penco, M. Petronio, L. Pivetta, M. Predonzani, F. Rossi, L. Rumiz, A. Salom, C. Scafuri, C. Serpico, P. Sigalotti, S. Spampinati, C. Spezzani, M. Svandrlik, C. Svetina, S. Zaccari, M. Trovo, R. Umer, A. Vascotto, M. Veronese, R. Visintini, M. Zaccaria, D. Zangrando, and M. Zangrando, *Nat. Photonics* **6**, 699 (2012).
- ²²E. Allaria, A. Battistoni, F. Bencivenga, R. Borghes, C. Callegari, F. Capotondi, D. Castronovo, P. Cinquegrana, D. Cocco, M. Coreno, P. Craievich, R. Cucini, F. D'Amico, M. B. Danailov, A. Demidovich, G. De Ninno, A. Di Cicco, S. Di Fonzo, M. Di Fraia, S. Di Mitri, B. Diviacco, W. M. Fawley, E. Ferrari, A. Filipponi, L. Froehlich, A. Gessini, E. Giangrisostomi, L. Giannessi, D. Giuresi, C. Grazioli, R. Gunnella, R. Ivanov, B. Mahieu, N. Mahne, C. Masciovacchio, I. P. Nikolov, G. Passos, E. Pedersoli, G. Penco, E. Principi, L. Raimondi, R. Sergo, P. Sigalotti, C. Spezzani, C. Svetina, M. Trovò, and M. Zangrando, *New J. Phys.* **14**, 113009 (2012).
- ²³E. Allaria, B. Diviacco, C. Callegari, P. Finetti, B. Mahieu, J. Viefhaus, M. Zangrando, G. De Ninno, G. Lambert, E. Ferrari, J. Buck, M. Iichen, B. Vodungbo, N. Mahne, C. Svetina, C. Spezzani, S. Di Mitri, G. Penco, M. Trovò, W. M. Fawley, P. R. Rebernik, D. Gauthier, C. Grazioli, M. Coreno, B. Ressel, A. Kivimäki, T. Mazza, L. Glaser, F. Scholz, F. Seltmann, P. Gessler, J. Grünert, A. De Fanis, M. Meyer, A. Knie, S. P. Moeller, L. Raimondi, F. Capotondi, E. Pedersoli, O. Plekan, M. B. Danailov, A. Demidovich, I. Nikolov, A. Abrami, J. Gautier, J. Lüning, P. Zeitoun, and Luca Giannessi, *Phys. Rev. X* **4**, 041040 (2014).
- ²⁴M. B. Danailov, F. Bencivenga, F. Capotondi, F. Casolari, P. Cinquegrana, A. Demidovich, E. Giangrisostomi, M. P. Kiskinova, G. Kurdi, M. Manfredda, C. Masciovecchio, R. Mincigrucci, I. P. Nikolov, E. Pedersoli, E. Principi, and P. Sigalotti, *Opt. Express* **22**, 12869 (2014).
- ²⁵F. Casolari, F. Bencivenga, F. Capotondi, E. Giangrisostomi, M. Manfredda, R. Mincigrucci, E. Pedersoli, E. Principi, C. Masciovecchio, and M. Kiskinova, *Appl. Phys. Lett.* **104**, 191104 (2014).
- ²⁶C. T. Chen, Y. U. Idzerda, H.-J. Lin, N. V. Smith, G. Meigs, E. Chaban, G. H. Ho, E. Pellegrin, and F. Sette, *Phys. Rev. Lett.* **75**, 152 (1995).
- ²⁷P. M. Oppeneer, in *Handbook of Magnetic Materials*, edited by K. H. J. Buschow (Elsevier, 2001), Vol. 13, p. 229.
- ²⁸J. Kuneš, P. M. Oppeneer, H.-Ch. Mertins, F. Schäfers, A. Gaupp, W. Gudat, and P. Novák, *Phys. Rev. B* **64**, 174417 (2001).
- ²⁹K. Carva, M. Battiato, and P. M. Oppeneer, *Nat. Phys.* **7**, 665 (2011).